

# Synthesis and characterization of optoelectronics bromoapatite $\text{Ca}_5(\text{PO}_4)_3\text{Br}:\text{RE}^{3+}$ ( $\text{RE}^{3+} = \text{Ce}^{3+}$ , $\text{Dy}^{3+}$ and $\text{Eu}^{3+}$ ) phosphors

V. V. Shinde, S. J. Dhoble\*

Department of Physics, R.T.M. Nagpur University, Nagpur 440033, India

\*Corresponding author. E-mail: [sjdhoble@rediffmail.com](mailto:sjdhoble@rediffmail.com)

Received: 14 October 2013, Revised: 27 March 2014 and Accepted: 10 April 2014

## ABSTRACT

The subject of this work is the characterization of the photoluminescence properties of  $\text{RE}^{3+}$  doped bromoapatite inorganic optoelectronic phosphor material. This paper reports the luminescence properties of  $\text{RE}^{3+}$  (Where  $\text{RE} = \text{Ce}$ ,  $\text{Dy}$ , and  $\text{Eu}$ ) doped  $\text{Ca}_5(\text{PO}_4)_3\text{Br}$ , which has been prepared by solid state reaction route. The prepared phosphor is well characterized by XRD, SEM, FT-IR and photoluminescence (PL) measurement. The apatite  $\text{Ca}_5(\text{PO}_4)_3\text{Br}:\text{Ce}^{3+}$  shows an efficient broad emission at 340 nm and weak 362 nm emission when excited at 293 nm.  $\text{Ca}_5(\text{PO}_4)_3\text{Br}:\text{Dy}^{3+}$  phosphor shows an efficient blue and yellow emissions at 485 nm and 577 nm respectively when excited at 390 nm.  $\text{Ca}_5(\text{PO}_4)_3\text{Br}:\text{Eu}^{3+}$  phosphor shows an orange and weak red emission at 592 nm and 615 nm respectively when excited at 396 nm. The effect of the  $\text{RE}^{3+}$  concentration on the luminescence properties of  $\text{Ca}_5(\text{PO}_4)_3\text{Br}:\text{RE}^{3+}$  phosphors are also studied. The investigated prepared bromoapatite phosphors may be suitable for a near UV excited LED. Copyright © 2014 VBRI Press

**Keywords:** Phosphor; apatite; photoluminescence; rare earth.



**V. V. Shinde** obtained M.Sc. degree in App. Electronics from S. G. Amraoti University, Amraoti, India in 1986. He is presently working as an Associate Professor in Department of Electronics, Jankidevi Bajaj College of Science, Wardha, India. During his research career, he is involved in the synthesis and characterization of solid state lighting nano materials. He is a member of Luminescence Society of India.



**S. J. Dhoble** obtained M.Sc. degree in Physics from Rani Durgavati University, Jabalpur, India in 1988. He obtained his Ph.D. degree in 1992 on Solid State Physics from Nagpur University, Nagpur. Dr. S. J. Dhoble is presently working as an Associate Professor in Department of Physics, R.T.M. Nagpur University, Nagpur, India. During his research career, he is involved in the synthesis and characterization of solid state lighting nanomaterials as well as development of radiation dosimetry phosphors using thermo-

luminescence, mechano-luminescence and lyo-luminescence techniques. Dr. Dhoble published several research papers in International reviewed journals on solid-state lighting, LEDs, radiation dosimetry and laser materials. He is an executive member of Luminescence Society of India.

## Introduction

Rare earth (RE) ions as luminescent centres with good optical efficiency are applied in many optoelectronics materials to prepare the optical devices. Recently, many researchers searched for novel optical materials that have low cost and interesting luminescent properties which may be helpful in solid state lighting and other display devices. Now a day white light emitting diodes LEDs are candidates for new lighting systems having number of advantages over conventional illumination devices including the incandescent and the fluorescent lamps in the view points of low electric consumption, high brightness, long lifetime and environment friendly [1].

At present, white LEDs composed of blue LEDs of indium gallium nitride (InGaN) and yttrium aluminium garnet (YAG) yellow phosphor at epoxy is commercialized [2, 3]. It has a critical disadvantage of low CRI (colour rendering index). To enhance luminescent properties, white LEDs composed of red, green, and blue (RGB) phosphors and nUV (near ultra-violet) LEDs are proposed instead of white LEDs organized with YAG yellow phosphors with InGaN based blue LEDs.

Recently, Dhoble et al. reported  $\text{Dy}^{3+}$  and  $\text{Eu}^{2+}$  activated  $\text{M}_5(\text{PO}_4)_3\text{F}$  (where  $\text{M} = \text{Ba}$ ,  $\text{Sr}$ ,  $\text{Ca}$ ) phosphors [4,5]. Also Ping Zhang et al. reported some new methods for the preparation of phosphate based phosphor, which are used in the commercial application [6]. A blue phosphor based on

phosphate host matrix was prepared by Wu et al. [7]. By introducing the  $Y^{3+}$  into  $Sr_2P_2O_7:Eu^{3+}$ , Pang et al. [8] successfully prepared a new phosphor with blue long-lasting emission by the high-temperature solid state reaction method.  $Eu^{3+}$ -doped triple phosphate  $Ca_3MgR(PO_4)_7$  ( $R = La, Gd, Y$ ) was synthesized by Haung et al. [9].

Some investigations are still going on novel apatite-based materials for its applications in various purposes such as making lamps, CR tubes and TV screens, electroluminescent lamp and display panels, LEDs, detectors for X-ray imaging, scintillation detectors, laser crystals, paints and solar concentrators. In this article we have reported the synthesis and characterisation of  $Ca_5(PO_4)_3Br$  doped with  $RE^{3+}$  (where  $RE^{3+} = Ce^{3+}, Dy^{3+}$  and  $Eu^{3+}$ ) by using the conventional solid state reaction method for the possible application in light emitting diodes.

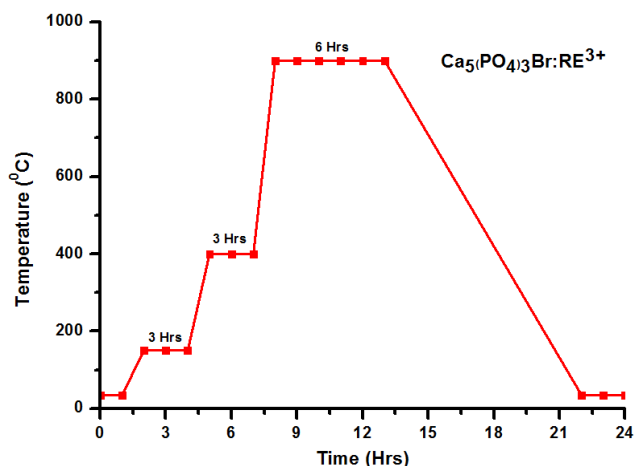
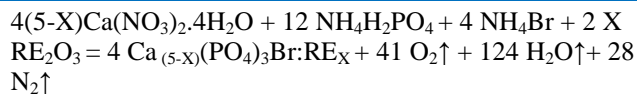
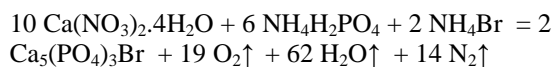


Fig. 1. Heating procedure for  $Ca_5(PO_4)_3Br$  phosphors prepared by using solid state reaction method.

## Experimental

Bromoapatite phosphors  $Ca_5(PO_4)_3Br$  reported here were prepared by the solid state reaction method. For the synthesis of  $Ca_5(PO_4)_3Br$  (pure) and  $Ca_5(PO_4)_3Br:RE^{3+}$  (where  $RE^{3+} = Ce^{3+}, Dy^{3+}$ , and  $Eu^{3+}$ ) bromoapatite phosphor,  $Ca(NO_3)_2 \cdot 4H_2O$ ,  $Sr(NO_3)_2$ ,  $NH_4H_2PO_4$ ,  $NH_4Br$  and  $(NH_4)_2Ce(NO_3)_6$ ,  $Dy_2O_3$ , and  $Eu_2O_3$  of annular grade were taken in stoichiometric ratio and were dry-mixed thoroughly by mechanical crushing for 1 h in agate mortar. These powders were then transferred to a silica crucible, annealed in a muffle furnace, at low temperature around  $150^\circ C$  for 3 hours. The powders were reground and again annealed at  $400^\circ C$  for 3 hours to wave off all gases. Again the powders were reground and finally annealed by slowly raising the temperature of muffle furnace, at about at  $1100^\circ C$  for 6 hrs. in air and then cooled down slowly to room temperature and reground, as done previously. Heating procedure for  $Ca_5(PO_4)_3Br:RE^{3+}$  phosphors prepared by using a solid-state reaction method is shown in Fig. 1.

The balanced chemical reaction for the formation of  $Ca_5(PO_4)_3Br$  (pure) and  $Ca_5(PO_4)_3Br:RE^{3+}$  are as follows:



where  $RE_2O_3 = Dy_2O_3$  and  $Eu_2O_3$ , for Ce doping  $(NH_4)_2[Ce(NO_3)_6]$  is used.

The phase purity and structure of the final products of the alkaline earth bromoapatite phosphors  $Ca_5(PO_4)_3Br$  was examined by x-ray powder diffraction using  $Cu K\alpha$  radiation on a BRUKER – analytical x-ray diffractometer. Phosphor morphology was observed by a Geol-6380A scanning electron microscope (SEM). Infrared spectra of the pure  $Ca_5(PO_4)_3Br$  was recorded on using a Bruker Fourier transform infrared spectrometer. For the measurement of spectroscopic properties, the excitation and emission spectra for all samples were recorded on Shimadzu make RF5301PC spectro-fluorometer using solid sample holder. Emission and excitation spectra were recorded using a spectral slit width of 1.5 nm at room temperature.

## Results and discussion

### X-ray diffraction

The prepared host lattice  $Ca_5(PO_4)_3Br$  was characterized for their phase purity and crystallinity by X-ray powder diffraction (XRD) at a scanning step size of 0.015, with a continuing step of 5 sec, in the 2 theta range from  $0^\circ$  to  $80^\circ$ . Fig. 2 shows the diffraction data pattern for the pure  $Ca_5(PO_4)_3Br$  phosphor. It shows good agreement with ICDD data file no. 74-0672. The XRD pattern did not indicate presence of the constituents  $Ca(NO_3)_2$  or  $NH_4Br$  or  $NH_4H_2PO_4$  and other likely phases. An excellent match is seen indicating formation of single phase, homogeneous final product  $Ca_5(PO_4)_3Br$  phosphor.

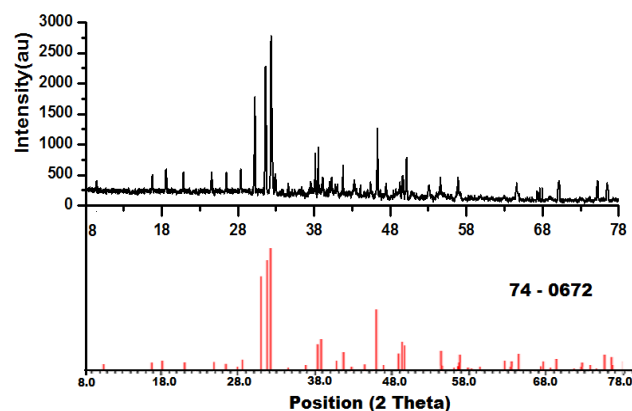


Fig. 2. XRD pattern of  $Ca_5(PO_4)_3Br$ .

A ball (sphere) model of crystalline structure of  $Ca_5(PO_4)_3Br$  phosphate is as shown in figure 3. The bromoapatite  $Ca_5(PO_4)_3Br$  belong to the large family of apatite structure compounds, that crystallize in the hexagonal system with the space group  $P6_3/m$ . The apatite structure is composed of isolated  $PO_4$  tetrahedra. Their spatial arrangement generates two cationic positions M(I) and M(II). M(I) cation are surrounded by  $PO_4$  tetrahedra

only, whereas M(II) cations are localized at the periphery of c-axis-oriented tunnels that also accommodate Br anions in a central position. For an apatite of formula  $[M(I)]_2[M(II)]_3[(PO_4)_3]Br$  crystallizing in the space group  $P_{63/m}$ , two cation sites can be considered for the rare-earth or alkaline-earth metals: M(I) (Wyckoff symbol 4f) and M(II) (Wyckoff symbol 6h). M(I) shows coordination number IX, with tricapped trigonal prismatic geometry, whereas M(II) shows coordination number VII, with pentagonal bipyramidal geometry as shown in Fig. 4.

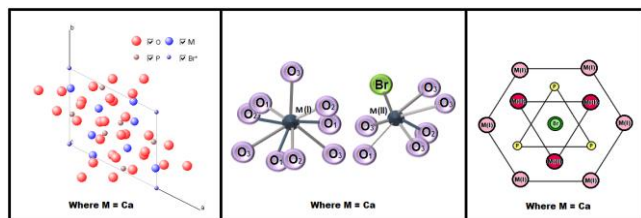


Fig. 3. Hexagonal crystal system of  $Ca_5(PO_4)_3Br$  phosphate.

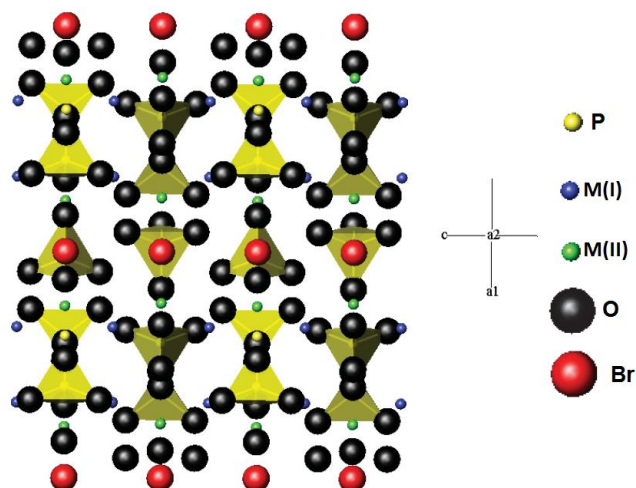


Fig. 4. Three-dimensional scheme of a bromoapatite  $M_5(PO_4)_3Br$  structure (Where  $M= Ca$ ) crystallizing in the  $P_{63/m}$  space-group.

### Surface morphology

Surface morphology of the phosphor was examined by using scanning electron microscopy (SEM, JED-2300) equipped with an energy dispersive spectrometry attached to the JEOL 6380A. The morphological images are presented in figure 5 showing micrographs for  $Ca_5(PO_4)_3Br$  phosphor materials. SEM observations of the sample show agglomerates ranging from few microns to a few tens of microns with highly porous morphology (Fig. 5a). Observations at higher magnification show the presence of highly agglomerated particles, with irregularly spherical morphology (Fig. 5b).

### FT-IR analysis

The spectrum for bromoapatite  $Ca_5(PO_4)_3Br$  phosphor is as shown in Fig. 6 below was taken in the range of 500 to 4000  $cm^{-1}$ . The most essential and the only polyatomic ion in bromoapatite is the phosphate group. A unit cell contains three phosphorous atoms and each phosphorous atom is surrounded by a tetrahedron of oxygen atoms.

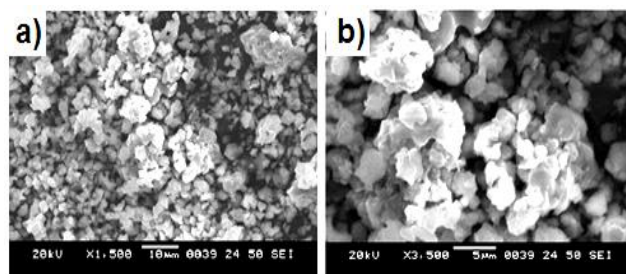


Fig. 5. SEM images taken at (a) low (500X) and (b) high (3500X) magnification of  $Ca_5(PO_4)_3Br$ .

The vibrational modes of the phosphate groups are the most prominent IR bands of bromoapatite. The absorption bands for  $Ca_5(PO_4)_3Br$  at 1026, 601, 567, 521 and 511  $cm^{-1}$  detected in the spectra are attributed  $(PO_4)^{3-}$  groups. These absorbance bands are possibly due to presence of various P–O bonds in the structure of  $Ca_5(PO_4)_3Br$ . The vibrational stretching region of IR spectrum indicates the identification of  $(PO_4)^{3-}$  bands. The major band at 1026  $cm^{-1}$  with shoulders around is identified as the antisymmetric stretching mode ( $\nu_3$ ) of phosphate oxyanion. The low-wavenumber region of IR spectrum shows four IR bands that are attributed to the symmetric bending modes ( $\nu_4$ ) of  $(PO_4)^{3-}$ . It can be further inferred that the powders are free of nitrate group (2213–2034  $cm^{-1}$ ). It is also observed that OH- bands completely disappeared in bromoapatite, suggesting that bromine ions have been substituted effectively. Thus characteristic bands of the  $(PO_4)^{3-}$  groups is observed.

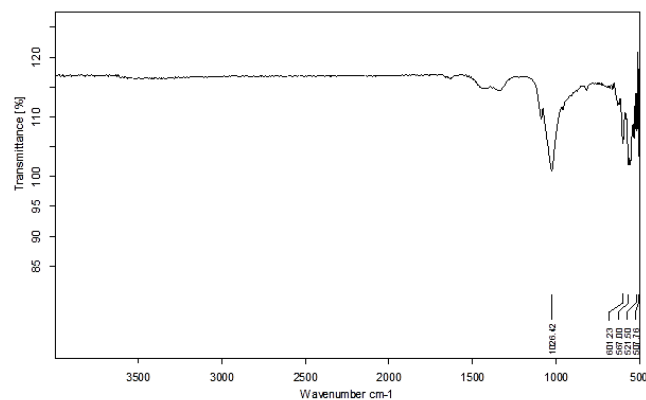


Fig. 6. FT-IR spectrum of synthesised  $Ca_5(PO_4)_3Br$  phosphor

### PL emission of $Ce^{3+}$ in $Ca_5(PO_4)_3Br$

Fig. 7 shows the excitation spectra in the 250–300 nm range and the emission spectra in the 315–500 nm range for samples  $Ca_{(5-x)}(PO_4)_3Br: Ce_x$  (where  $X = 0.5, 1, 2, 5,$  and 10 mole %) at room temperature. The excitation spectrum is obtained by monitoring the emission at 340 nm. The broad band is observed at around 263 nm with prominent shoulder at around 293 nm at room temperature. The excitation bands at 263 nm and 293 nm are assigned to the lowest 4f–5d transition for  $Ce^{3+}$  in the host lattice. The promotion of an electron from the  $^4F$  to the  $^5D$  orbital is due to lowest energy transition of  $Ce^{3+}$ . All transitions of  $Ce^{3+}$  are spin-allowed because the ground state and the excited

states of this  ${}^4F$  ion are spin doublets. Therefore, the excitation peak appears in the UV spectral region at 263 nm with prominent shoulder at around 293 nm at room temperature. More than one  $4F-5D$  excitation bands shows that the crystal field might have split the excited state ( ${}^5D_1$ ) into two components indicating that  $Ce^{3+}$  ions occupy more than one lattice site [10].

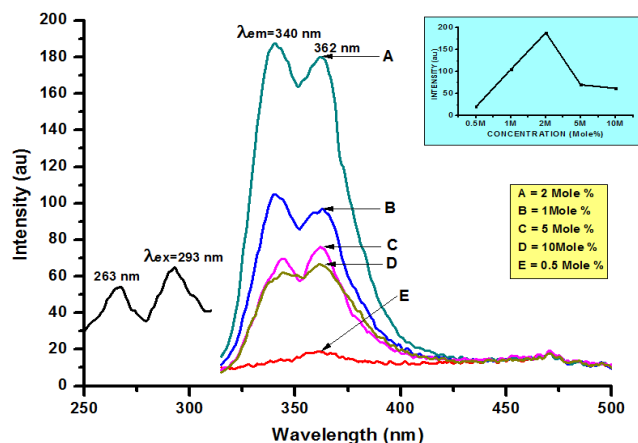


Fig. 7. Excitation and emission spectra of  $Ca_5(PO_4)_3Br:Ce^{3+}$  phosphor.

The PL emission spectra of  $Ce^{3+}$  ions in  $Ca_5(PO_4)_3Br$  (For mole % = 0.5, 1, 2, 5 and 10) phosphors with different concentrations under the excitation of 293 nm wavelengths of light is as shown in Fig. 7. A strong peak is observed at 340 nm and weak peak is noticed at 362 nm which are assigned to the  $5d-4f$  transition of  $Ce^{3+}$  ions. The dominant emission at 340 nm on 293 nm excitation is attributed to  $Ce^{3+}$  ions located at  $Ca^{2+}$  sites without local charge compensation. The weak emission at 362 nm is ascribed to  $Ce^{3+}$  ions located at  $Ca^{2+}$  sites in association with charge compensatory vacancy. From the two peaks observed at 340 nm and at 362 nm, it is clear that the emission bands correspond to the  $5d-4f$  transition of  $Ce^{3+}$  ions. The excited state derived from the  $5d$  state is sensitive to the crystal field and is coupled to the lattice vibrations which results in broader band emission rather than line emission. Normally  $Ce^{3+}$  emission shows two bands due to the doublet character of the  $4f$  ground state ( ${}^2F_{5/2}$  and  ${}^2F_{7/2}$ ). The emission appears in UV range and is more intense and broader in all  $Ce^{3+}$  activated  $Ca_5(PO_4)_3Br$  phosphors. It is also noticed that the peak positions of the emission bands for all  $Ce^{3+}$  doped  $Ca_5(PO_4)_3Br$  have not changed [11-14].

When luminescence intensities at different activator concentration are compared, it is seen that for small doping at 1 and 2 mole %, strong luminescence at 340 nm is observed compared to 362 nm but at 5 and 10 mole% the intensity of 362 nm emission is stronger than 340 nm peak. This is because the ionic radii of  $Ca^{2+}$  and  $Ce^{3+}$  ions in seven-fold coordinated system are 106 and 107 pm and 118 and 119 pm in nine-fold coordinated system, respectively [15]. Clearly the radii of  $Ca^{2+}$  and  $Ce^{3+}$  are almost similar to each other in both seven and nine-fold coordination system. Therefore  $Ce^{3+}$  ions can enter either Ca(I) or Ca(II) sites. From results, we can conclude that  $Ce^{3+}$  ions enter Ca(II) sites preferentially at low concentration and occupy Ca(I) sites at higher concentration.

As the concentration of  $Ce^{3+}$  ion increases the corresponding intensity of peaks also increases up to 2 mole % as shown in inset of Fig. 7 and later on decreases at higher concentration. This indicates a change in the surrounding of the  $Ce^{3+}$  ions at higher concentration in the  $Ca_5(PO_4)_3Br$  lattice which tends fluorescence intensity to quench. This may be due to energy transfer between the  $Ce^{3+}$  ions and defects of the  $Ca_5(PO_4)_3Br$  host and/or due to cross relaxation between the  $Ce^{3+}$  ions [16].

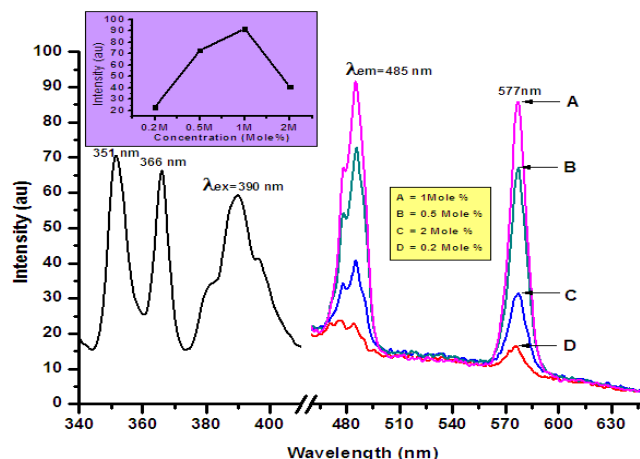


Fig. 8. Excitation and emission spectra of  $Ca_5(PO_4)_3Br:Dy^{3+}$  phosphor.

#### PL emission of $Dy^{3+}$ in $Ca_5(PO_4)_3Br$

The photoluminescence excitation spectra of the prepared  $Dy^{3+}$  activated  $Ca_5(PO_4)_3Br$  phosphor in the range 340 to 410 nm for different concentrations of  $Dy^{3+}$  ion monitored at 485 nm emission are shown in Fig. 8. The excitation peaks observed at 351 nm, 366 nm and 390 nm are due to transitions from ground level,  ${}^6H_{15/2}$  to higher energy levels  ${}^6P_{7/2}$ ,  ${}^6P_{5/2}$ , and  ${}^4I_{13/2}$  of  $Dy^{3+}$  ion, respectively. Amongst these three near UV excitation peaks, we chose 390 nm as excitation wavelength because it is more suitable for solid state lighting.

The emission spectra of  $Ca_5(PO_4)_3Br:Dy^{3+}$  (For mole % = 0.2, 0.5, 1 and 2) phosphors excited at 390 nm display two dominant peaks at 485 nm (blue) and at 577 nm (yellow). These blue and yellow emissions can be attributed to the electronic transitions of  ${}^4F_{9/2} \rightarrow {}^6H_{15/2}$  and  ${}^4F_{9/2} \rightarrow {}^6H_{13/2}$  respectively [17]. The blue emission is due to magnetic dipole transition, and the yellow emission belongs to the hypersensitive (forced electric dipole) transition following the selection rule,  $\Delta J = 2$ . In the studied  $Ca_5(PO_4)_3Br: Dy^{3+}$  phosphors, the intensity of blue emission is greater than that of the yellow emission. It is well known that the magnetic dipole transition ( ${}^4F_{9/2} \rightarrow {}^6H_{15/2}$ ) is insensitive to the crystal field around the  $Dy^{3+}$  ions and the hyper sensitive transition ( ${}^4F_{9/2} \rightarrow {}^6H_{13/2}$ ) is strongly influenced by the outside environment surrounding of  $Dy^{3+}$ . When  $Dy^{3+}$  is at a high symmetry site (with inversion symmetry), the blue emission is stronger than the yellow one [18-20]. When  $Dy^{3+}$  is located at a low symmetry site (without inversion symmetry), the yellow emission is dominant in the emission spectrum. In this  $Ca_5(PO_4)_3Br$  host, the stronger blue emission indicates that  $Dy^{3+}$  ions take the site with inversion symmetry.

The inset of **Fig. 8** shows the dependence of the luminescence intensity on doping ion  $\text{Dy}^{3+}$  concentration. The emission spectra shape does not vary with the  $\text{Dy}^{3+}$  concentration but the luminescence intensity changes more significantly. It is found that the emission intensity of  $\text{Dy}^{3+}$  increases with an increase of doping ion concentration. It reaches to a maximum value at 1 mole %, and then decreases with an increase of doping at 2 mole % due to typical property named concentration quenching. This is due to when the concentration of  $\text{Dy}^{3+}$  continues to increase, the interaction among them increases and leads to self-quench and therefore the emission intensity decreases. The concentration quenching of  $\text{Dy}^{3+}$  luminescence is mainly caused by cross-relaxation, i.e. energy transfers from one  $\text{Dy}^{3+}$  to another neighbour  $\text{Dy}^{3+}$  by transition that match in energy [21].

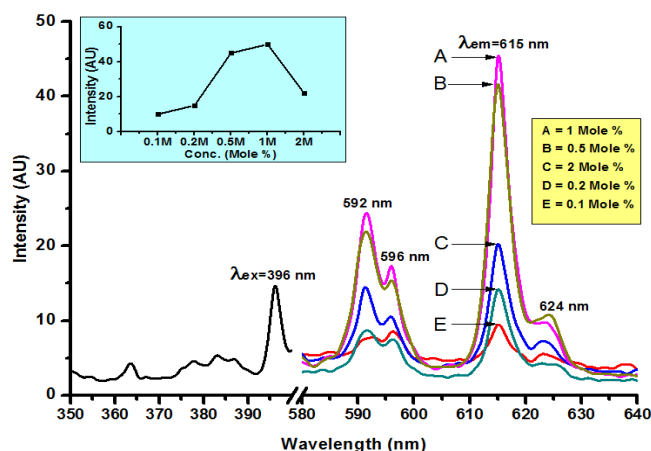


**Fig. 9.** Excitation and emission spectra of  $\text{Ca}_5(\text{PO}_4)_3\text{Br}:\text{Eu}^{3+}$  phosphor.

#### PL emission of $\text{Eu}^{3+}$ in $\text{Ca}_5(\text{PO}_4)_3\text{Br}$

The **Fig. 9** shows photoluminescence excitation spectrum of the prepared  $\text{Eu}^{3+}$  activated  $\text{Ca}_5(\text{PO}_4)_3\text{Br}$  phosphor by monitoring the red emission in the range 610 - 615 nm. The excitation band is observed at 396 nm ( ${}^7\text{F}_0 \rightarrow {}^5\text{L}_6$ ) is sharp and caused by f-f transition. One of the interesting results of this work is that the excitation spectrum of the  $\text{Ca}_5(\text{PO}_4)_3\text{Br}$  phosphor could be strongly excited by a near UV radiation, which has the potential as a near-UV LED converted phosphor in solid state lighting technology.

The emission spectra of  $\text{Ca}_5(\text{PO}_4)_3\text{Br}:\text{Eu}^{3+}$  (For mole % = 0.1, 0.2, 0.5, 1 and 2) phosphor have been obtained with excitations at 396 nm and is as shown in **Fig. 9**. With  $\lambda_{\text{ex}} = 396$  nm, emissions are more intense at 615 nm than at 592 nm in  $\text{Ca}_5(\text{PO}_4)_3\text{Br}:\text{Eu}^{3+}$ . The characteristic emission bands of  $\text{Ca}_5(\text{PO}_4)_3\text{Br}:\text{Eu}^{3+}$  phosphor are in region of 580 to 640 nm and corresponds to intra 4f-shell transitions of  ${}^5\text{D}_0 \rightarrow {}^7\text{F}_1$  ( $J=0, 1, 2, 3, 4$ ) of  $\text{Eu}^{3+}$ . A strong red emission of  $\text{Eu}^{3+}$  in the region 613-625 nm was obtained due to the  ${}^5\text{D}_0 \rightarrow {}^7\text{F}_2$  transition, along with emissions in the region 590 to 596 nm due to  ${}^5\text{D}_0 \rightarrow {}^7\text{F}_1$  transition.

The luminescence spectra of  $\text{Eu}^{3+}$  ion is slightly influenced by surrounding ligands of the host material because the transition of  $\text{Eu}^{3+}$  involve only a redistribution of electrons within the inner 4f subshells [22-23]. A few, however, are sensitive to the environment and become more intense and such transitions are known as hypersensitive

transitions. For  $\text{Ca}_5(\text{PO}_4)_3\text{Br}:\text{Eu}^{3+}$  phosphor the emission in the range 610 - 615 nm due to  ${}^5\text{D}_0 \rightarrow {}^7\text{F}_2$  is electric dipole transition and is considered as a hypersensitive transition [24], which obeys the selection rule of  $\Delta J=2$  and hence it is a bright emission. The transition in the range 590 to 596 nm due to  ${}^5\text{D}_0 \rightarrow {}^7\text{F}_1$  is equally bright orange emission with the selection rule  $\Delta J=1$  is a magnetic-dipole transition. Further, if  $\text{Eu}^{3+}$  occupies an inversion symmetry site in the host matrix, then the orange emission from 590 to 596 nm ( ${}^5\text{D}_0 \rightarrow {}^7\text{F}_1$ ) could be a dominant one. On the contrary, if  $\text{Eu}^{3+}$  does not occupy the inversion symmetry site, the transition  ${}^5\text{D}_0 \rightarrow {}^7\text{F}_2$  would be a dominant. In  $\text{Ca}_5(\text{PO}_4)_3\text{Br}:\text{Eu}^{3+}$  phosphor, emission in the range 610 - 615 nm is more intense and bright and hence we can infer that  $\text{Eu}^{3+}$  ions did not occupied the inversion symmetry site when the phosphor is excited at  $\lambda_{\text{ex}} = 396$  nm [25-26].

The emission intensity is related to the concentration of the  $\text{Eu}^{3+}$  activator ions. With the increase of concentration of the  $\text{Eu}^{3+}$  ion, the distance between  $\text{Eu}^{3+}$  ions becomes less and this results in the migration of excitation energy among  $\text{Eu}^{3+}$  ions leading to quenching of the emission. The highest luminescent intensity is obtained at 1mole% as shown in inset of figure 9 and then declines with the increase in concentration of the  $\text{Eu}^{3+}$  activator ions.

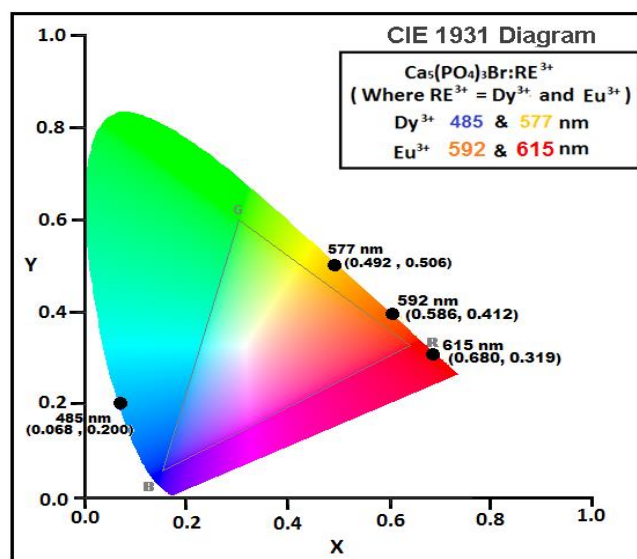


**Fig. 10.** Chromatic graph of  $\text{Ca}_5(\text{PO}_4)_3\text{Br}:\text{RE}^{3+}$  (where  $\text{RE}^{3+} = \text{Dy}^{3+}$  and  $\text{Eu}^{3+}$ ) phosphor excited near UV excitation.

**Table 1.** CIE Co-ordinates of  $\text{Pb}_5(\text{PO}_4)_3\text{Br}:\text{RE}^{3+}$  phosphor.

PHOSPHOR	EXCITATION (nm)	STRONG EMISSION (nm)	(X,Y) CO-ORDINATE	COLOUR REGION
$\text{Ca}_5(\text{PO}_4)_3\text{Br}:\text{Dy}^{3+}$	390	485	(0.068, 0.200)	Blue
		577	(0.492, 0.506)	Yellow
$\text{Ca}_5(\text{PO}_4)_3\text{Br}:\text{Eu}^{3+}$	397	592	(0.586, 0.412)	
		615	(0.680, 0.319)	Red

#### Chromatic properties

The **Fig. 10** shows the Commission International de l'Eclairage (CIE) chromaticity co-ordinates of the prepared phosphor  $\text{Ca}_5(\text{PO}_4)_3\text{Br}:\text{Dy}^{3+}$  and  $\text{Ca}_5(\text{PO}_4)_3\text{Br}:\text{Eu}^{3+}$ . The chromatic co-ordinates (X, Y) are calculated using the

colour calculator radiant imaging software and are summarized in following **Table 1** [27].

### Conclusion

Reported here bromide based alkaline earth metal halo phosphates, also known as bromoapatite,  $\text{Ca}_5(\text{PO}_4)_3\text{Br}:\text{RE}^{3+}$  (Where  $\text{RE}^{3+} = \text{Ce}^{3+}$ ,  $\text{Dy}^{3+}$  and  $\text{Eu}^{3+}$ ) optoelectronics phosphor has been prepared by the solid state diffusion. PL properties in the near UV and visible region which are characteristics for optoelectronic devices are studied. XRD analysis is carried out to study phase purity of the prepared optoelectronics phosphor. SEM analysis show agglomerates ranging from few microns to a few tens of microns with highly porous morphology of the synthesised phosphor. FT-IR shows the M-O vibrations in  $\text{Ca}_5(\text{PO}_4)_3\text{Br}$  host lattice at different frequencies. CIE study is carried out to study colour quality. The developed  $\text{Ca}_5(\text{PO}_4)_3\text{Br}:\text{RE}^{3+}$  phosphor has been excited in near UV range which is desirable characteristics for commercially available W-LED. The developed phosphor emits in the blue, yellow and red and hence has the potential to be used in phosphor converted LED as a primary colour emitter in 3 band pc-LED or red spectrum enhancer in yellow phosphor converted white LED and therefore our results indicate that prepared phosphor may be a promising candidates for white LEDs.

### Reference

1. S. Nakamura, T. Mukai, M. Senoh, *Appl. Phys. Lett.* **1994**, *64*, 1687.  
DOI: [10.1063/1.111832](https://doi.org/10.1063/1.111832).
2. G. Blasse, A. Bril, *Appl. Phys. Lett.* **2000**, *11*, 53.  
DOI: [10.1063/1.1755025](https://doi.org/10.1063/1.1755025)
3. T. Tamura, T. Setomoto, T. Taguchi, *J. Lumin.* **2000**, *87-89*, 1180.  
DOI: [10.1016/S0022-2313\(99\)00588-8](https://doi.org/10.1016/S0022-2313(99)00588-8)
4. Nagpure, I.M.; Shinde, K.N.; Dhoble, S.J.; Kumar, Animesh; *J. Alloys and Compd.* **2009**, *481*.  
DOI: [10.1016/j.jallcom.2009.03.069](https://doi.org/10.1016/j.jallcom.2009.03.069)
5. Shinde, K.N.; Dhoble, S.J.; *Adv. Mat. Lett.* **2010**, *1*(3), 254.  
DOI: [10.5185/amlett.2010.9161](https://doi.org/10.5185/amlett.2010.9161)
6. Zhang, P.; Li, L.; Xub, M.; Liu, L. *J. Alloys Compd.* **2008**, *456*, 216.  
DOI: [10.1016/j.jallcom.2007.02.004](https://doi.org/10.1016/j.jallcom.2007.02.004)
7. Wu, Z.; Liu, J.; Gong, M. *Chem. Phys. Lett.* **2008**, *466*, 88.  
DOI: <http://dx.doi.org/10.1063/1.4754449>
8. Pang, R.; Li, C.; Shi, L.; Su, Q. *J. Phys. and Chem. of Solids* **2009**, *70*, 303.  
DOI: [10.5185/amlett.2010.9161](https://doi.org/10.5185/amlett.2010.9161)
9. Huang, Y.; Jiang, C.; Cao, Y.; Shi, L.; Seo, H. *J. Mat. Resea. Bull.* **2009**, *44*, 793.  
DOI: [10.1364/OE.19.0000A1](https://doi.org/10.1364/OE.19.0000A1)
10. Y.Q. Li, G. de With, H.T. Hintzen, *J. Lumin.* **2006**, *116*, 107.  
DOI: [10.1016/j.jlumin.2005.03.014](https://doi.org/10.1016/j.jlumin.2005.03.014)
11. R. Le Toquin, A.K. Cheetham, *Chemical Physics Letters* **2006**, *423*, 352–356.  
DOI: [10.1016/j.cplett.2006.03.056](https://doi.org/10.1016/j.cplett.2006.03.056)
12. K. N. Shinde, S. J. Dhoble and K. Park, *Nano-Micro Lett.* **2012**, *4*(2), 78.  
DOI: [10.3786/nml.v4i2.p78-82](https://doi.org/10.3786/nml.v4i2.p78-82)
13. S. J. Dhoble, K. N. Shinde, *Adv. Mat. Lett.* **2011**, *2*(5), 349.  
DOI: [10.5185/amlett.2011.3072am2011](https://doi.org/10.5185/amlett.2011.3072am2011)
14. Jianhui Zhang, Hongbin Liang, Ruijin Yu, Haibin Yuan, Qiang Su, *Materials Chemistry and Physics* **2009**, *114*, 242.  
DOI: [10.1016/j.matchemphys.2008.09.045](https://doi.org/10.1016/j.matchemphys.2008.09.045)
15. P. Dorenbos, *Phys. Rev. B* **2001**, *64*, 125117.  
DOI: [10.1103/PhysRevB.64.125117](https://doi.org/10.1103/PhysRevB.64.125117)
16. Janai'na Gomes Æ Osvaldo Antonio Serra, *J. Mater. Sci.* **2008**, *43*, 5460.  
DOI: [10.1007/s10853-007-1777-5](https://doi.org/10.1007/s10853-007-1777-5)
17. K. N. Shinde, S. J. Dhoble, *Adv. Mat. Lett.* **2010**, *1*(3), 254.  
DOI: [0.5185/amlett.2010.9161](https://doi.org/10.5185/amlett.2010.9161)
18. Zhao, D.; Lin, Z.; Zhang, L.; Wang, G. *J. Cryst Growth*, **2007**, *299-1*,

223.  
DOI: [10.1016/j.jcrysgro.2006.11.239](https://doi.org/10.1016/j.jcrysgro.2006.11.239)
19. Zeng, Q.; Liang, H.; Gong, M.; Su, Q. *J. Electrochem. Soc.*, **2008**, *155*, H730.  
DOI: [10.1149/1.2965527](https://doi.org/10.1149/1.2965527)
20. Wang, Z.; Liang, H.; Wang, Q.; Lou L.; Gong M.; *Mat. Sci.* **2009**, *164*, 120.  
DOI: [10.1016/j.mseb.2009.08.002](https://doi.org/10.1016/j.mseb.2009.08.002)
21. Brixner, L.H.; *Mater. Res. Bull.*, **1974**, *9*, 1041.  
DOI: [10.1016/0025-5408\(74\)90014-2](https://doi.org/10.1016/0025-5408(74)90014-2)
22. [22] Shinde, K.N.; Dhoble, S.J., *Adv. Mat. Lett.* **2010**, *1*(3), 254.  
DOI: [10.5185/amlett.2010.9161](https://doi.org/10.5185/amlett.2010.9161)
23. [23] Yu-Ming Peng a,b, Yan-Kuin Su a,b, Ru-Yuan Yang, *Materials Research Bulletin* **2013** *48*, 1946..  
DOI: [10.1016/j.materresbull.2013.01.039](https://doi.org/10.1016/j.materresbull.2013.01.039)
24. Abhay D. Deshmukh, S. J. Dhoble, N.S. Dhoble, *Adv. Mat. Lett.* **2011**, *2*(1), 38.  
DOI: [10.5185/amlett.2010.10171](https://doi.org/10.5185/amlett.2010.10171)
25. Zhang, C. X., Jiang, W. J., Yang, X. J. et al., *J. Alloys Comp.*, **2009**, *474*, 287.  
DOI: [10.1016/j.jallcom.2008.06.061](https://doi.org/10.1016/j.jallcom.2008.06.061)
26. Suresh.K., Murthy,KVR., Atchyutha Rao,Ch., Poornachandra Rao,N.V and Subba Rao,B, *J. Lumin.*, **2012**.  
DOI: [10.1016/j.jlumin.2011.12.045](https://doi.org/10.1016/j.jlumin.2011.12.045)
27. Color Calculator version 2, software from Radiant Imaging, Inc, **2007**.



## ***Advanced Materials Letters***

### **Publish your article in this journal**

[ADVANCED MATERIALS Letters](#) is an international journal published quarterly. The journal is intended to provide top-quality peer-reviewed research papers in the fascinating field of materials science particularly in the area of structure, synthesis and processing, characterization, advanced-state properties, and applications of materials. All articles are indexed on various databases including [DOAJ](#) and are available for download for free. The manuscript management system is completely electronic and has fast and fair peer-review process. The journal includes review articles, research articles, notes, letter to editor and short communications.

